Available online at www.sciencedirect.com
SCIENCE DIRECT
ELSEVIER
Journal of Electrostatics 64 (2006) 361–367
Journal of ELECTROSTATICS
www.elsevier.com/locate/elstat

Minimizing the torque ripple of variable capacitance electrostatic micromotors

V. Behjat*, A. Vahedi

Department of Electrical Engineering, Iran University of Science and Technology, Iran

Received 6 October 2004; received in revised form 1 August 2005; accepted 8 September 2005
Available online 10 October 2005

Abstract

In this paper, an approach for minimizing the torque ripple of a variable capacitance electrostatic micromotor is presented. To this end, a practical design for a variable capacitance electrostatic micromotor has been analyzed using a two-dimensional, numerical, finite element method. The procedure presented here for minimizing the torque ripple consists of two stages: optimization of the excitation sequence and optimization of the geometric parameters. Several excitation sequences have been studied for minimizing the torque ripple, and the optimal excitation sequence has been found for supplying the micromotor. Geometric parameters are optimized to minimize torque ripple. The geometric optimization procedure is based on the successive sampling of geometric parameters. These parameters include stator tooth width, rotor tooth width and slot radius.

Keywords: Electrostatic micromotor; Torque ripple; Geometric parameter; Field analysis; Finite element method

1. Introduction

The greatest promise of microelectromechanical systems (MEMS) lies in their ability to produce mechanical motion on a very small scale [1]. A variety of techniques for achieving microactuation have been developed, including electrostatic, electromagnetic, ultrasonic, hydraulic and thermal methods. Of these, electrostatic micromotors are commonly used due to their simplicity of fabrication. The electrostatic micromotor is less affected by scaling and from the fabrication point of view, it can be easily integrated on a chip, because all fabrication processes are compatible with traditional IC fabrication processes [2]. Possible applications for the electrostatic micromotors are growing rapidly, especially for problems in optics and electronics [3–5].

Two types of electrostatic micromotors have already been studied and built: variable capacitance electrostatic micromotors and electric induction micromotors. The first variable capacitance electrostatic micromotors with diameters of 60–120 μm were developed by Fan et al. in 1989 at the University of California at Berkeley [5]. Frechette et al. successfully realized the first electrostatic induction micromotor supported on gas-lubricated bearings in 2001 [4]. The variable capacitance principle is commonly used due to its simple construction and smaller material requirements.

The electrostatic torque produced in variable capacitance electrostatic micromotor has both average and ripple components. One problem with electrostatic micromotors is that they exhibit pulsating torque, and the ripple component of the torque can be a considerable percentage of the overall torque. Hence it is difficult to achieve large average torques. To generate the large average torques needed in many applications, an optimal excitation sequence and an optimal motor geometry are required.

In order to appraise the electrostatic torque, the electrostatic field must first be evaluated. To this end, we have used a finite element method (FEM) to analyze the electrostatic field.

2. Variable capacitance electrostatic micromotor

After realization of the first electrostatic micromotor, electrostatic micromotors have been produced in many

*Corresponding author.
E-mail addresses: Vahid_Behjat@ee.iust.ac.ir (V. Behjat), avahedi@iust.ac.ir (A. Vahedi).

0304-3886/$ - see front matter
doi:10.1016/j.elstat.2005.09.003

laboratories. The study reported in this paper has been performed on a practical design of a variable capacitance electrostatic micromotor that was prototyped at the Massachusetts Institute of Technology [6]; Fig. 1 shows the longitudinal view of the "MIT" prototype. The surface micromachining of polysilicon has been applied to the fabrication of the micromotor.

In the schematic drawing of the micromotor in Fig. 1, the micromotor is been shown prior to release. The latter is the stage at which the low-temperature oxide (LTO) layers are dissolved in hydrofluoric acid (HF) to release the rotor. Micromotor structural components (groundplane, rotor and stator, hub holding the rotor) are fabricated from heavily phosphorous-doped polysilicon. After release, the rotor is supported on its bushings and is free to rotate about the center-pin bearing contacting the electric shield under the rotor. During micromotor operation, the rotor is intended to be in electrical contact with the shield positioned beneath it through the mechanical contact at the bearing or at the bushing supports [7].

The rotor and stator are made from polysilicon films, while the medium between them is air. This micromotor is called a variable capacitance, side-drive micromotor, because it uses the electrostatic force which occurs between the edges of the rotor and the stator.

The operation principle is very simple. The micromotor operates based on the electrostatic forces that tend to align the rotor poles with the excited stator poles. Once the stator poles are activated, the rotor teeth tend to be aligned with the active stator poles to minimize the field energy. In operation, stator electrodes are switched on and off, one after the other.

The electrostatic forces acting on the micromotor are exerted in the three major directions: axial, radial and tangential [8]. In order to maximize the driving torque, high tangential forces are desirable, whereas axial and radial components should be minimized. To avoid radial forces on the rotor, the micromotor is driven by applying DC voltage to radially opposing pairs of stator electrodes.

The cross-section of the micromotor being investigated in this study has been shown in Fig. 2. The micromotor has 12 stator electrodes and 8 rotor teeth. The angular width of stator and rotor electrodes, τ_s and τ_r, respectively, are equal to 18°, while their pole pitch angles, τ_{ps} and τ_{pr}, respectively, are 30°, 45°. The gap δ between rotor and stator is 1.5 μm. The radius r_1 of the rotor, is equal to 50 μm. The inner diameter of the rotor, r_3, is equal to 21 μm. The slot radius of the micromotor, r_2, is equal to 30 μm and finally, the axial thickness of the rotor and stator is 2.2 μm. Table 1, summarizes the geometric parameters.

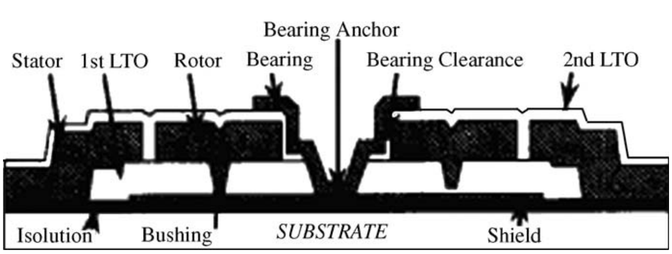

Fig. 1. Longitudinal view of the completed side-drive micromotor.

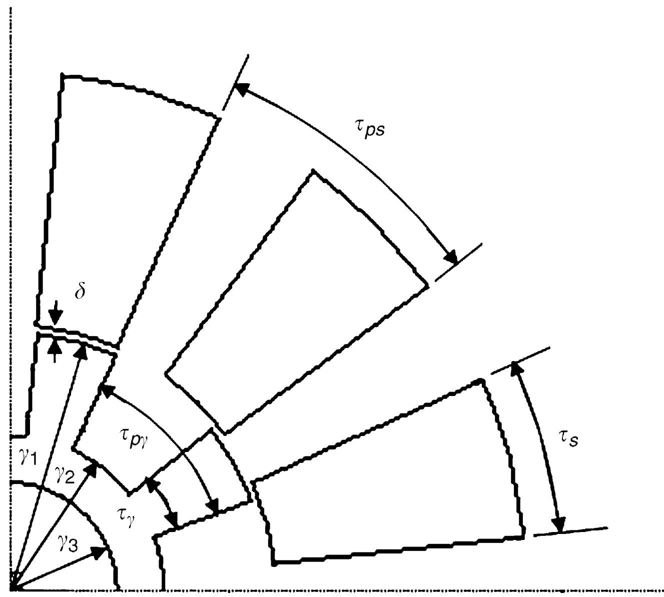

Fig. 2. Cross-section view (one quarter) of the electrostatic micromotor.

Table 1
Geometric parameters

Parameter	Symbol	Quantity
Stator pole pitch	τ_{ps}	30°
Rotor pole pitch	τ_{pr}	45°
Stator tooth width	τ_s	18°
Rotor tooth width	τ_r	18°
Rotor radius	r_1	50 μm
Slot radius	r_2	30 μm
Inner radius of the rotor	r_3	21 μm
Gap spacing	δ	1.5 μm
Axial thickness	h	2.2 μm

Electrical breakdown for devices with micron gaps smaller than 5 μm is different from the well-known Paschen's law that describes the gaseous breakdown voltage as a function of the reduced variable of the pressure-gap spacing product.

For gaps grater than about 10 μm, breakdown occurs when the electric field exceeds about 3 V/μm. Wallash and colleagues showed that electrical breakdown for gap spacing smaller than 5 μm does not follow Paschen's law. Instead the field strength at breakdown in this range is on the order of 75 V/μm. Fig. 3 shows the modified Paschen curve for air at 1 atm.

Moving from 10 μm to smaller gaps, the modified Paschen curve shows a plateau where the pure Paschen curve would have a minimum [9,10].